Depsidones from Lichens as Natural Product Inhibitors of M-Phase Phosphoprotein 1 (MPP1), a Human Kinesin Required for Cytokinesis

Sandeep K. Talapatra,[*,†,‡] Oliver Rath,[‡] Eddie Clayton,[∥] Sophie Tomasi,[§] and Frank Kozielski[*,†]

[†] The School of Pharmacy, University College London, Department of Pharmaceutical and Biological Chemistry, 29-39 Brunswick Square, London WC1N 1AX, UK

[‡] The Beatson Institute for Cancer Research, Garscube Estate, Switchback Road, Glasgow G61 1BD, Scotland, UK

[§] Equipe PNSCM "Produits naturels - Synthèses - Chimie Médicinale", Unités Mixtes de Recherche, Centre National de la Recherche Scientifique, 6226 Sciences chimiques de Rennes, UFR Sciences Pharmaceutiques et Biologiques, Univ. Rennes 1, Université Européenne de Bretagne, 2 Avenue du Pr. Léon Bernard, F-35043 Rennes, France

[∥] Cyprotex Discovery Ltd, 15 Beech Lane, Macclesfield, Cheshire SK10 2DR, UK

ABSTRACT

M-Phase Phosphoprotein 1 (MPP1), a microtubule plus end directed kinesin, is required for the completion of cytokinesis. Previous studies have shown that MPP1 is upregulated in various types of bladder cancer. This article describes inhibitor-screening leading to the identification of a new class of natural product inhibitors of MPP1. Two compounds with structural similarity, norlobaridone (**1**) and physodic acid (**2**) were found to inhibit MPP1. Physodic acid is not competitive with ATP, indicating the presence of an allosteric inhibitor-binding pocket. Initial drug-like property screening indicates that physodic acid is more soluble than norlobaridone and has more favorable lipophilicity. However both suffer from high clearance in human microsomal stability assays mediated by the liability of the lactone ring as well as hydroxylation of the alkyl chains as shown by metabolite identification studies. In cell-based assays physodic acid is a weak inhibitor with GI_{50} values of about 30 µM in a range of tumor cell lines. The two depsidones identified and characterized here could be used for future improvement of their activity against MPP1 and will be useful chemical probes for studying this unique molecular motor in more depth.

Molecular motors of the kinesin superfamily move along microtubule (MT) tracks to perform a diverse set of functions from intracellular transport to cell division.[1] Among the 45 different kinesins expressed in humans, the majority is involved in intracellular trafficking processes, whereas about 16 kinesins are implicated in mitosis and cytokinesis.[2,3] The kinesin-6 family consists of three members, named Mitotic Kinesin-Like Protein 1 (MKLP-1, also known as Kif23), Mitotic Kinesin-Like Protein 2 (MKLP-2, also known as Kif20A, Rabk6, Rabkinesin-6 or Rab6-KIFL) and M-Phase Phosphoprotein 1 (MPP1, also known as Kif20B, KRMP1 or MPHOSPH1), which are predominantly involved in cytokinesis, although report suggest they play non-redundant roles.[3-5] Members of the kinesin-6 family are unique amongst the kinesin superfamily, because they contain an exceptionally long insertion (8 - 10 kDa) of unknown function in the loop L6 region of the motor domain.[6,7]

In contrast to MKLP-1 and MKLP-2 that have been studied intensively, at least in tumor cell lines, there is only very limited information available for the third member of the kinesin-6 family, MPP1. Through genome sequencing projects, MPP1 has been identified in at least 13 eukaryotic species including human, rat, mouse and Xenopus. Human MPP1 is a slow MTs plus-end-directed molecular motor necessary for the completion of cytokinesis.[3] Particular structural features include the long loop L6 in the motor domain and a particularly long neck-linker region.[3] This protein has been shown to be regulated *in vivo* by posttranslational modification through phosphorylation in the carboxyl-terminal tail domain at Thr1604 by cdc2 kinase.[8] MPP1 has been reported to interact with the mitotic peptidyl-prolyl isomerase (Pin1) *in vivo* and that this interaction is mediated through the tail domain of MPP1 and the amino-terminal WW domain of Pin1. Another interacting partner is protein regulator of cytokinesis 1 (PRC1).[9] MPP1's ATPase activity is stimulated by MTs and MPP1 shows MT-bundling activity. In HCT116 colon carcinoma cells, depletion of MPP1 by RNAi leads to defects during cytokinesis, which can result in apoptotic cell death.[3] Interestingly, cell death seems to occur through two different mechanisms: in the first mechanism, the midbody of RNAi treated cells "persists" without abscission and the two physically connected daughter cells undergo apoptosis. In the second mechanism, the midbody regresses leading to the appearance of binucleated cells with subsequent apoptosis. In contrast, in another study,

in which MPP1 was depleted in HeLa cells, the authors did not detect any significant defects in cytokinesis.[10] The mRNA of MPP1 has been shown to be significantly upregulated in bladder cancer (and in a variety of bladder cancer tumor cell lines) as well as large B cell lymphoma.[9,11] In total, MPP1's interaction with PRC1 and its subsequent implication in bladder carcinogenesis makes MPP1 a potential target for bladder cancer drug development.[12]

2-Phenylquinoxalines[13] have been reported as small molecule inhibitors of MPP1 but the patent has subsequently been withdrawn. In this project small molecule libraries from the NCI were screened for the inhibition of the ATPase activity of human MPP1. The aim of this study was to identify novel MPP1-specific inhibitors that can be used as chemical probes for studying MPP1 biology and as potential lead compounds for drug development. In this paper the recombinant expression, purification and biochemical characterization of two human MPP1 motor domain constructs are described. It also reports the discovery and characterization of an MPP1-specific inhibitor, originally isolated from lichens, known as depsidones that was identified using an *in vitro* inhibitor screening assay. MPP1-inhibitor interaction and investigation of the effect on different tumor cell lines including bladder, colon, pancreatic and leukemia cell lines were subsequently characterized. In addition, some basic drug-like properties of the MPP1-specific inhibitor were also characterized. In conclusion this paper describes the identification and characterization of an MPP1-specific inhibitor (Figure 1A and 1B) that can be used to study the biochemical and structural features of human MPP1. However, further development is necessary to improve its physico-chemical properties and potency.

RESULTS AND DISCUSSION

Characterization of MPP1 Motor Domain Constructs. Human MPP1 is a protein of 1853 residues (Figure 2A). It contains a short N-terminal sequence of unknown function preceding the motor domain (aa 1 to 56), followed by the motor domain (aa 56 to 491) which includes a large loop L6 insertion (aa 186 to 262) (Figure 2B), a particularly long discontinuous coiled coil region (aa 568 to 1600) and a C-terminal tail domain (aa 1602 to 1853) (Figure 2A). Two MPP1 constructs, coding for residues 2 to 477, which also include the small N-terminal domain (residues 2 to 56) preceding the motor domain and residues 57 to 491 (subsequently named $MPP1_{2-477}$ throughout the manuscript) and a protein covering the entire MPP1 motor domain (named $MPP1_{57-491}$) but lacking the first 56 residues, were cloned into an *E. coli* expression vector and were expressed and purified to homogeneity. Mass spectrometry finger print analyses with sequence coverage of 56% and 77% respectively confirmed that the two purified proteins were indeed human MPP1. Gel filtration analysis revealed that $MPP1_{2-477}$ (51 kDa) and $MPP1_{57-491}$ (43 kDa) are both monomeric in solution (data not shown).

To optimize and miniaturize the experimental conditions for inhibitor screening and subsequent biochemical assays, the basic kinetic parameters of $MPP1_{2-477}$ and $MPP1_{57-491}$ were first investigated (Table 1 and Figure 3). We used two different constructs, one including the small 56 residues long N-terminal domain adjacent to the motor domain and the second construct lacking this domain (Figure 2A). Our aim was to identify whether the N-terminal small domain would have an effect on the overall kinetic properties of the MPP1 motor domain and whether this N-terminal domain would be involved in inhibitor binding or not.

Determination of the salt-dependence of the basal ATPase activity was performed by measuring the k_{cat} in the presence of increasing NaCl concentrations. The activity decreases with increasing salt concentration indicating that the basal MPP1 ATPase activity is best measured in the absence of salt for both motor domain constructs (Figure 3A). The basal ATPase activity in the presence of increasing ATP concentrations, in the absence of salt led to a maximum k_{cat} of 0.016 ± 0.001 s^{-1} with a $K_{M,ATP}$ of 68.5 ± 16 μM for $MPP1_{2-477}$ and the k_{cat} for $MPP1_{57-491}$ is 0.010 ± 0.001 s^{-1} with a $K_{M,ATP}$ of 128 ± 2.1 (Figure 3B). Subsequently, MT-stimulated k_{cat} as well as the $K_{M,ATP}$ and $K_{0.5,MT}$ in the

4

presence of MTs were measured. The k_{cat} values of the MT-stimulated ATPase activities are 3.1 ± 0.2 s^{-1} and 4.1 ± 0.1 s^{-1} for MPP1$_{2-477}$ and MPP1$_{57-491}$, respectively, corresponding to 193-fold and 410-fold stimulations compared to the basal ATPase activities. The $K_{M,ATP}$ values are 44 ± 4 µM and 82 ± 2 µM (Figure 3C) and the $K_{0.5,MT}$ values are 102 ± 3 nM and 112 ± 1 nM for MPP1$_{2-477}$ and MPP1$_{57-491}$, respectively (Figure 3D). We conclude from the above data that the absence or presence of the small N-terminal head domain preceeding the motor domain does not significantly affect the kinetic properties of MPP1. Therefore, we decided to use MPP1$_{57-491}$, which could be expressed in larger amounts than MPP1$_{2-477}$ for further inhibitor screening.

Inhibitor Screening and Hit Identification. Based on these results, initial screening of MPP1$_{57-491}$ for inhibitors was conducted by observing the inhibition of the basal ATPase activity in the absence of salt and in the presence of 1 mM Mg^{2+}ATP, using several small molecule libraries from the NCI including the mechanistic, the structural diversity and the natural product sets. One initial hit was the depsidone norlobaridone (**1**), a natural product originally isolated from *Xanthoparmelia conspersa* and *X. scabrosa* (Figure 1).[14] To verify the initial hit obtained in the library the powder was obtained from the NCI/NIH and its activity MPP1$_{57-491}$ was quantified. Norlobaridone (**1**) inhibits the basal MPP1 ATPase activity with an IC$_{50}$ of 18.7 ± 2.6 µM and the MT-stimulated ATPase activity with an IC$_{50}$ of 24.4 ± 3.5 µM indicating that it is a weak inhibitor of MPP1. An analogue, physodic acid (**2**), tested thereafter was more active than **1** inhibiting the basal and MT-stimulated ATPase activities with IC$_{50}$ values of 9.9 ± 1.1 µM and 5.8 ± 0.9 µM, respectively (Figure 4). To exclude the possibility of aggregation based inhibition[15], the inhibition of the basal ATPase activity of both **1** and **2** were measured in the presence of 0.1% Tween-20 to reduce compound aggregation. The IC$_{50}$ values obtained for both the inhibitors were similar to those obtained without detergent (data not shown). Interestingly, MPP1$_{2-477}$, which contains the small N-terminal domain preceding the motor domain, is inhibited by both depsidones to a larger extend than the shorter MPP1 construct (Table 2). The depsidone variolaric acid (**3**), which contains an additional five-membered ring system but lacks the alkyl chains, is inactive. **1** and **2**

contain two alkyl substituents, which might contribute towards their activity against MPP1 ATPase activity.

The compounds were then tested in proliferation assays using HCT116 (colon), Bx-PC-3 (pancreatic), K562 (leukemia) and J82 as well as UM-UC-3 (both bladder cancer) cell lines (Table 3). The well-known Eg5 inhibitor STLC (**4**) was used as a control. Interestingly, **1** and **2**, displayed a measurable effect in the panel of cell lines tested with GI_{50} values ranging between 31.8 to 48.3 µM. **3** did not show any measurable effects in the concentration range tested.

Determination of the Type of Inhibition for MPP1 in the Absence or Presence of MTs. The type of inhibition for **2**, was then determined for the more potent analogue. In the absence of MTs, **2** is an un-competitive inhibitor of MPP1 with respect to ATP (Figure 5A), as indicated by decreasing V_{max} and K_m values. In the presence of MTs, **2** is a mixed inhibitor (a special case of non-competitive inhibition) of MPP1 with respect to ATP (Figure 5B) as observed by an increase in apparaent K_m but a decrease in the apparent V_{max} when the $K_{m,ATP}$ is measured at increasing concentrations of **2**. On the other hand **2** is non-competitive with respect to MTs (Figure 5C) as the apparent K_m remains the same whereas V_{max} decreases with increasing inhibitor concentrations.

Determining the Specificity of Physodic acid (2) within the Kinesin Superfamily. The specificity of **2** was measured for MPP1 by investigating the possible inhibition of the ATPase activity of human kinesins from different subfamilies (Table 4). **2** was specific for human MPP1 as it did not significantly inhibit any other mitotic kinesins of the kinesin-6 family or other kinesins involved in mitosis or cytokinesis, for example Eg5 (kinesin-5)[16], Kif15[17] (kinesin-12), or MKLP-2[18]/MKLP-1 (kinesin-6). Compound **2** also did not inhibit the activity of two kinesins involved in intracellular transport, Kif7[19]/Kif27 (kinesin-7) and Kif5a/Kif5b (kinesin-1). Partial inhibition of between 40% and 50% at 200 µM for Kif4 and Kif9 were observed, for which no IC_{50} value could be calculated. The compound also showed partial inhibition of between 60% and 70% for both the basal and MT-stimulated ATPase activity of the kinetochore motor CENP-E with IC_{50} values of 29.6 ± 12.7 µM and 91.4 ± 31.0 µM, respectively.

Profiling of Drug-Like Properties. The determination of basic drug-like properties provided important insights into ADME characteristics of **1** and **2** (Table 5). Both compounds show pH-dependent solubility, which rises with increasing pH. Whereas **1** shows only partial solubility at pH 7.4, **2** has good solubility probably due to the presence of an additional carboxylic acid group. The $logD_{7.4}$ (the distribution coefficient at a pH of 7.4) of 3.0 for **2** is slightly more favorable than for norlobaridone ($logD_{7.4}$ = 3.5). In PAMPA assays, which investigate passive diffusion, **1** showed some passive permeability whereas **2** did not display any permeability. The bi-directional Caco-2 permeability assay was used to determine the compound efflux ratio. Whereas **2** did not give satisfactory results, the efflux ration for **1** was 0.51 indicating that no drug efflux occurs. Subsequent testing of both compounds in human and mouse microsomal stability assays showed high clearance in human and mouse microsomal stability assays with half-life times of only 3.5 and 4.5 min in human microsomes and 3.1 min and 22.5 min in mouse microsomes for **1** and **2**, respectively. In both human and mouse microsomal stability assays, physodic acid showed low values in the control without cofactor, which indicates either chemical instability or non-cofactor dependent enzymatic degradation. Compound **2** was therefore tested in chemical stability assays and was shown to be stable, although it showed some minor unspecific binding to polypropylene. In addition, assays performed in the absence of microsomes for both compounds indicated that they were chemically stable. This points to a non-NADPH-dependent enzymatic process in the microsomes, that also contributes to some clearance, but which was not investigated further. To further investigate the high clearance observed for depsidones compound **2** was incubated with human liver microsomes and the resulting metabolites identified by mass spectrometry. Three metabolic pathways were found by LC-MS and the relationship of the products to **1** was determined by their collision induced mass spectra (see the Supplementary Material Section for details). They were hydrolysis of the lactone ring (-CO_2- to –CO_2H HO-) metabolite M1, oxidation of the pentyl side chain (C_5H_{11} to $C_5H_{10}OH$) M2 and further cleavage of the phenolic ether M3 (methyl 2,4 dihydroxy -6 pentanoylbenzoate).

Discussion. There is a continuous need to identify and validate novel potential drug targets. Certain human mitotic kinesins are considered as potential mitotic spindle targets for drug development in cancer chemotherapy. Not surprisingly, several clinical candidates, leads or chemical probes targeting a variety of human kinesins have been reported including Eg5[20], CENP-E[21], Kif18b[22], MKLP-2[23], MCAK[24] and KifC1[25,26]. Drug candidates targeting Eg5 and CENP-E are in clinical phase I and II trials[27,28],[28] and the most promising compound, ARRY-520, has proven effective in refractory and relapsed multiple myeloma in combination with a proteasome inhibitor. One potential novel candidate is MPP1 from the kinesin-6 family. This unusual motor protein has previously been shown to move towards the plus-end of MTs and is involved in cytokinesis.[3] MPP1 has also been reported to be phosphorylated during mitosis at its C-terminus, which is crucial for its role in cytokinesis.[8] Importantly, previous literature also suggests the importance of MPP1 overexpression in progressive and invasive forms of bladder cancer.[9] These initial findings suggest that MPP1 may serve as a potential drug candidate for targeting bladder cancer and specific chemical probes against MPP1 may serve to further validate this early hypothesis.

A patent[13] reported specific MPP1 inhibitors known as 2-phenylquinoxalines (**6**) (Figure 1). There was a marked phenotype of bineculated cells in BSC-1 (African green monkey) cells treated with these inhibitors, but unfortunately, the patent was later withdrawn.

In order to identify novel inhibitors of MPP1, two MPP1 motor domains were first cloned, expressed and purified with subsequent characterization of their kinetic parameters (Table 1). The analysis confirmed similarities with other motor domain from different kinesins like Eg5[29,30], Kif15[17] and Ncd[30]. Thereafter, in order to identify potential inhibitors of MPP1, in vitro screening using previously established procedures was performed.[31] Reported here is the identification and initial characterization of two closely related natural product inhibitors of MPP1, **1** and **2** acid from a class of compounds known as depsidones derived from lichens.

Having demonstrated that **2** is a low micro molar inhibitor of MPP1, the type of

inhibition was characterized thereafter. The results show that **2** is a un-competitive inhibitor with respect to ATP under basal and a mixed inhibitor when measured in the presence of MTs and is a non-competitive inhibitor with respect to MTs. Since depsidones do not compete with ATP or MTs, MPP1 must also contain at least one allosteric inhibitor-binding pocket, as observed in other kinesins for example Eg5, CENP-E and KifC1.

Lichens are symbiotic organisms composed of algae or cyanobacteria and fungi. Morethan 1,000 compounds have been isolated from different lichens, which have been estimated to comprise almost 20,000 species. Many of the secondary metabolites that have been identified so far are unique to lichens. Lichen metabolites have been shown to possess a range of interesting biological properties including antioxidant, antimicrobial, antiherbivore and insecticidal activities.[32] Several natural products from lichens have been shown to possess cytotoxic activity[33] and for a few isolated lichen metabolites growth inhibition and apoptotic cell death has been reported.[34,35] One interesting class of lichen compounds is represented by depsidones containing the dibenzodioxepinone scaffold (Figure 1) and for which a number of structurally related derivatives have been isolated and characterized from a variety of lichen species.[36] Cytotoxic activity has been observed for several chlorinated depsidones[35] and botryosphaerones.[37] In most cases, the biological targets that are inhibited are unknown. Therefore, the identification of the target(s) for these compounds will open the way of their use as chemical probes to study the function of these proteins, to further validate their potential as therapeutic targets and in the best case improve their chemical scaffolds for drug development. Compound **4** has recently been shown to inhibit tubulin polymerization[38] and MPP1 is a novel cytoskeletal protein target to be identified for the class of compounds known as depsidones. A structurally related depsidone, Corynesidone A (Figure 1), extracted from the fungus *Corynespora cassicola* L36, is a known aromatase inhibitor.[39]

In this study it was also observed that in cell based assays, **2** is effective with GI_{50} values of around 30 μM in bladder cancer cell lines. Although cell-based activity is only weak, this is in line with previous finding where MPP1 has been found to be overexpressed in various bladder cancer cell lines. Though the initial compounds display low potency in tumor cell lines, further development, particularly with regard to

improving the metabolic liabilities of the compounds and optimizing their drug-like properties, may increase their efficacy. A major problem is the lack of metabolic stability of both depsidones with half lifes of only several minutes in human and mouse microsomal stability assays (Table 5). The subsequent metabolite identification study for compound **2** revealed the Achilles' heel of this type of compound, which will have to be taken into account for further optimization: the major metabolites originated from hydrolysis of the lactone ring metabolite M1, or hydroxylation of the alkyl chain (C_5H_{11} to $C_5H_{10}OH$) metabolite M2, and finally cleavage of the ether bond of metabolite M1 to give M3.

In conclusion, further optimization of potency coupled with efficacy in tumor cell lines to study MPP1 function will require the substitution and/or stabilization of the labile lactone ring and removal or shortening of the alkyl chains, if these substituents are not required for activity against MPP1. Reducing the length of the alkyl chains would also have the additional advantage of reducing lipophilicity (clogP) and increase solubility of the analogues in aqueous solution.

In summary, a low micromolar natural product inhibitor, physodic acid (**2**), has been reported here that targets MPP1 identified using an in vitro screening method. The inhibitor is specific for MPP1 compared to other kinesins but displays some drug like property liabilities such as high metabolic clearance and low cell permeability. This novel MPP1 inhibitor can be used as a chemical probe to study MPP1 either biochemically, biophysically or structurally. In particular a crystal structure of the depsidone-MPP1-$Mg^{2+}ADP$ ternary complex would be useful to understand the interactions in molecular detail. Further improvement of the scaffold will focus on studying analogues of available depsidones to identify analogues with improved potency and drug-like properties.

EXPERIMENTAL SECTION

Chemicals. The small molecule libraries for inhibitor screening were obtained from the NCI/NIH. Norlobaridone (**1**, NSC31867) and physodic acid (**2**, NSC5916) were obtained from the NCI/NIH (Rockville, USA). Variolaric acid (**3**) was obtained from Produits Naturels, Syntheses et Chimie Medicinal (PNSCM, S. Tomasi). Norlobaridone

and variolaric acid have a purity of >95%, whereas the purity of physodic acid is 94%, as shown by LC-MS.

Physodic acid. White amorphous powder; IR (KBr): v_{max} = 2400-3300, 1692, 1660, 1616 cm^{-1}; HRESIMS: m/z = 493.1838 [M + Na]$^+$ (calcd. for $C_{26}H_{30}O_8Na$: 493.1842); ^{1}H-NMR and ^{13}C-NMR identical to published data.[40]

Variolaric acid. White powder; IR (KBr): $v$max = 3410, 3060, 1748, 1727, 1626, 1577 cm^{-1}; HRESIMS m/z 314.0430 [M]$^{+.}$ (calcd for $C_{16}H_{10}O_7$ 314.0427); ^{1}H NMR (270 MHz, DMSO-d_6) and ^{13}C NMR (67.5 MHz, DMSO-d_6) data comparable to published values[40].

Initial Drug-Like Property Profiling and Metabolite Identification.
Turbidimetric solubility, $log_{D7.4}$, and human as well as mouse microsomal stability were determined as previously described.[41] PAMPA, Caco-2 and chemical stability assays were carried out at Cyprotex according to internal protocols, including all necessary controls.

Cloning, Expression and Purification of Human MPP1 Constructs. The motor domain of human MPP1$_{2-447}$ and MPP1$_{57-491}$ were cloned in ppSUMO (with an N-terminal SUMO fusion and His$_6$-tag) expression plasmid. The primers (Sigma) for the two different constructs are as follows: MPP1$_{2-447}$: Forward Primer: 5'-GCC ATT GCA CAA TAA GTT TGT GTC CCA GAC-3'; Reverse Primer: 5'-GTC TGG GAC ACA AAC TTA TTG TGC AAT GGC-3'; MPP1$_{57-491}$: Forward Primer: 5'-GAA CAG ATT GGT GGA TGC GGA TCC AAA GAT TAT CTC AGG TT-3'; Reverse Primer: 5'-CTT GAG AGG AAT TTA AAG TGT CTT AGA CAC AAA CTT TTT GTG-3'. The cloning strategy and the sequences were verified by DNA sequencing.

For protein expression and purification, plasmids were transformed into *Escherichia coli* BL21 CodonPlus (Novagen, Watford, UK). 12 L of bacterial culture were grown at 37 °C in TB (Terrific Broth) medium supplemented with 100 mg/l ampicillin to an A_{600} of 0.7 and induced overnight with 0.5 mM IPTG (Isopropyl β-D-thiogalactoside; Melford, Chelsworth, UK) at 20 °C. Harvested cells were resuspended in buffer A [50 mM PIPES pH 6.8, 1 mM MgCl$_2$, 1 mM Na-EGTA, 250 mM NaCl and 10 mM imidazole] supplemented with 1 mM PMSF, 1 mM Mg^{2+}ATP and 2.5 mg of lysozyme, and subjected to one cycle of freeze–thaw and sonication, before 1 mM DNaseI was added.

The lysate was centrifuged for 1 h in a J25 (Beckman, High Wycombe, UK) rotor at 30000 g at 4 °C.

Clear lysates were loaded on to a 5 ml HisTrap FF column (GE Healthcare, Buckinghamshire, UK) equilibrated in buffer A. The resin was washed with buffer A containing 10 mM imidazole and the proteins were eluted on a gradient of buffer B [50 mM Pipes pH 6.8, 1 mM $MgCl_2$, 1 mM Na-EGTA, 250 mM NaCl and 1 M imidazole]. Fractions containing the protein were pooled and the buffer was exchanged for desalting buffer C [50 mM PIPES pH 6.8, 250 mM NaCl, 1 mM $MgCl_2$ and 1 mM Na-EGTA]. Ulp1 protease purified as previously shown[42], 1 mM Mg^{2+}ATP and 1 mM $MgCl_2$ were added and reaction mixtures were incubated overnight at 4 °C. Uncleaved proteins and protease were removed by running the sample through the His-trap column for a second time. The cleaved protein was diluted using buffer D [50 mM PIPES pH 6.8, 1 mM $MgCl_2$ and 1 mM Na-EGTA] to obtain a final salt concentration of ~30 mM. The diluted sample was then applied to a 5 ml Hitrap FF (GE Healthcare, Buckinghamshire, UK) ion-exchange column to remove the remaining contaminants. The protein was eluted with a gradient of buffer E [50 mM PIPES pH 6.8, 1 mM $MgCl_2$, 1 mM Na-EGTA and 250 mM NaCl]. The protein containing fractions were pooled and run through a final step of size-exclusion chromatography on a Superdex 75 column (GE Healthcare, Buckinghamshire, UK) equilibrated in gel-filtration buffer F [50 mM PIPES pH 6.8, 200 mM NaCl, 1 mM DTT, 1 mM Na-EGTA and 1 mM $MgCl_2$].

The protein obtained was pooled and concentrated on an Amicon ultrafiltration device (Millipore, Watford, UK) to a final concentration of approx. 2-3 mg/ml and flash frozen in liquid nitrogen and stored at -80 °C after adding 5% glycerol. The proteins have been used freshly purified where possible with occasional use of frozen proteins.

Steady State ATPase Measurements and Determination of IC_{50} Values. Steady-state basal and MT-stimulated ATPase rates were measured using the pyruvate kinase/lactate dehydrogenase-linked assay.[43] The amounts of MPP1 constructs were optimized to 680 nM for the basal and 50 nM for the MT-stimulated activity assays. For $K_{m,ATP}$, the concentration of ATP was within a range from 0 mM to 2 mM for both basal and MT-stimulated ATPase assays, whereas MTs were used in the range of 0 µM to 20 µM for the determination of the $K_{m,MTs}$. Kinetics measurements were carried out at 25 °C

using a 96-well Sunrise photometer (TECAN, Maennesdorf, Switzerland). The data were analyzed using Kaleidagraph 4.0 (Synergy Software, Reading, UK). The kinetic parameters k_{cat}, $K_{m, ATP}$, $K_{m, MTs}$ were initially calculated and optimized based on the rates computed from equation 1.

$$s^{-1} = \Delta A/min \times 2 / (\varepsilon_{NADH} \times 60 \times C_{enzyme}) \ldots\ldots\ldots\ldots eq. \ 1$$

where, (ε_{NADH} corresponds to the molar extinction coefficient of NADH (6220 $\Delta A/mol/cm$), $\Delta A/min$ is the absorbance decrease at 340 nm per min, and C_{enzyme} is the molar concentration of MPP1 used in the assay. The factor 2 is a correcting factor taking into account the length of the optical path in the 96-well plate, normalized to a path of 1 cm. The IC_{50} values for the inhibition of the basal and MT-stimulated ATPase activities of MPP1 were calculated for depsidones analogues at concentrations ranging from 0 µM to 200 µM.

Determination of the Type of Inhibition of Physodic Acid for MPP1 in the Absence and Presence of MTs. The type of inhibition for the depsidones in the absence and presence of MTs was determined based on the steady state ATPase measurements as described above. Compound **2** was the more potent compound and was selected for these assays. The V_{max} and K_m of ATP in the absence and presence of MTs and for MTs (at a constant ATP concentration) were measured to decipher the type of inhibition. For the determination of the type of inhibition with respect to ATP in the absence of MTs, ATP was used at a concentration range from 0 to 2 mM for each individual inhibitor concentration at 0, 1, 5, 10 and 20 µM.

The type of inhibition with respect to ATP in the presence of MTs was determin- ed at an MPP1 concentration of 50 nM and a fixed MT concentration of 1 µM. The inhibitor concentrations investigated were 0, 1, 5 10 and 20 µM with either increasing concentration of ATP from 0 mM to 2 mM.
The type of inhibition with respect to MTs was determined at an MPP1 concentration of 50 nM and a fixed ATP concentration of 1 mM using MT concentrations between 0 and 1 µM.

For measurement of specificity of **2** against a set of kinesins the protein concentr- ations used ranged from 200 nM to 800 nM for basal ATPase activity assays and 5 nM to 90 nM for MT-stimulated ATPase assays. The inhibitor concentration for each kinesin is

measured in the range of 0 to 200 μM. The graph fitting was done with GraphPad Prism 5.01 for Windows (GraphPad Software, San Diego, USA).

Measurement of EC_{50} for Human Cancer Cells Lines for the Depsidones. HTC116 (ATCC CCL-247) cells were cultured in DMEM (Invitrogen, Paisley, UK), supplemented with 10% fetal bovine serum (PAA, Pasching, Austria). K562 (ATC CCCL-243) cells were cultured in RPMI (Invitrogen, Paisley, UK), supplemented with 10% fetal bovine serum (PAA, Pasching, Austria). J82 (ATCC HTB-1) and UM-UC-3 (ATCC CRL-1749) cells were cultured in Advanced MEM (Invitrogen, Paisley, UK), supplemented with 10% fetal bovine serum (PAA, Pasching, Austria). BxPC-3 (ATCC CRL-1687) cells were cultured in RPMI (Invitrogen, Paisley, UK), supplemented with 1% nonessential amino acids (Invitrogen, Paisley, UK), 1% sodium pyruvate (Invitrogen, Paisley, UK), 1% glutamine (Invitrogen, Paisley, UK) and 10% fetal bovine serum (PAA, Pasching, Austria). All cells were maintained at 37 °C, 95% humidity, and 5% carbon dioxide in a humidified incubator. They were used for experiments for 6-8 weeks before they were replaced with fresh stocks, which are stored in liquid nitrogen.

Cell Proliferation Assays. All compounds were tested to determine their growth inhibition effect (EC_{50}) in the human leukemic cell line K562, the colon cancer cell line HCT116 and the two bladder cancer cell lines J82 and UM-UC-3, respectively. Experimental procedures were as previously described.[44]

Briefly, cells were seeded in triplicate in 96-well assay plates at 1.250 cells (HCT116), 2.000 cells (J82, UM-UC-3), or 5.000 cells (K562) per well in 100 μL of the respective growth medium. Medium blanks (without any cells) and cell blanks (without any inhibitors) for every cell line were also prepared. On the next day, inhibitors were added with a starting concentration of 100 μM in a 3-fold serial dilution series. After 72 h post inhibitor addition, 10% Alamar Blue (Invitrogen, Paisley, UK) was added and depending on the cell line, 2-12 h later the absorbance was measured at 570 and 600 nm. All values were corrected for the absorbance of the medium blank and the corrected cell blanks were set to 100%. Calculations for determining the relative proliferation were performed using equations described in the manufacturer's manual. Finally, the EC_{50} values were determined using a sigmoidal dose-response fitting (variable slope) with GraphPad Prism 5.01 for Windows (GraphPad Software, San Diego, USA).

AUTHOR INFORMATION

Corresponding Authors

*Tel: +44 207 753 5879. E-mail: f.kozielski@ucl.ac.uk

*Tel: +44 207 753 5918. E-mail: s.talapatra@ucl.ac.uk

Notes

The authors declare no competing financial interest

ASSOCIATED CONTENT

*S Supporting Information
The Supporting Information is available free of charge on the ACS Publications website.

> Identification of metabolites and LC-MS/MS data of norlobaridone along with cid spectrum of norlobaridone and its metabolites

REFERENCES

(1)   Hirokawa, N.; Noda, Y.; Tanaka, Y.; Niwa, S. *Nat. Rev. Mol. Cell Biol.* **2009**, *10*, 682-696.

(2)   Rath, O.; Kozielski, F. *Nat. Rev. Cancer* **2012**, *12*, 527-539.

(3)   Abaza, A.; Soleilhac, J. M.; Westendorf, J.; Piel, M.; Crevel, I.; Roux, A.; Pirollet, F. *J. Biol. Chem.* **2003**, *278*, 27844-27852.

(4)   Gruneberg, U.; Neef, R.; Honda, R.; Nigg, E. A.; Barr, F. A. *J. Cell Biol.* **2004**, *166*, 167-172.

(5)   Kuriyama, R.; Dragas-Granoic, S.; Maekawa, T.; Vassilev, A.; Khodjakov, A.; Kobayashi, H. *J. Cell Sci.* **1994**, *107 (Pt 12)*, 3485-3499.

(6)   Miki, H.; Okada, Y.; Hirokawa, N. *Trends Cell Biol.* **2005**, *15*, 467-476.

(7)   Wade, R. H. *Structure* **2002**, *10*, 1329-1336.

(8)   Kamimoto, T.; Zama, T.; Aoki, R.; Muro, Y.; Hagiwara, M. *J. Biol. Chem.* **2001**, *276*, 37520-37528.

(9)   Kanehira, M.; Katagiri, T.; Shimo, A.; Takata, R.; Shuin, T.; Miki, T.; Fujioka, T.; Nakamura, Y. *Caner Res.* **2007**, *67*, 3276-3285.

(10)   Zhu, C.; Zhao, J.; Bibikova, M.; Leverson, J. D.; Bossy-Wetzel, E.; Fan, J. B.; Abraham, R. T.; Jiang, W. *Mol. Biol. Cell* **2005**, *16*, 3187-3199.

(11)   Nishiu, M.; Yanagawa, R.; Nakatsuka, S.; Yao, M.; Tsunoda, T.; Nakamura, Y.; Aozasa, K. *Jpn. J. Cancer Res.* **2002**, *93*, 894-901.

(12)   Baron, R. D.; Barr, F. A. In *Book The Kinesin-6 Members MKLP1, MKLP2 and MPP1*; Kozielski, F., Ed.;Springer Netherlands, 2015, 12, pp193-222.

(13)   Nigg, E. A.; Mayer, T. U.; Huemmer, S.; Barr, F. A.; Bormann, J.,EP1683523 A1, 2006.

(14)   Culberson, C. F.;Chemical and Botanical Guide to Lichen Products, 1969

(15)   Feng, B. Y.; Simeonov, A.; Jadhav, A.; Babaoglu, K.; Inglese, J.; Shoichet, B. K.; Austin, C. P. *J. Med. Chem.* **2007**, *50*, 2385-2390.

(16)   Talapatra, S. K.; Anthony, N. G.; Mackay, S. P.; Kozielski, F. *J. Med. Chem.* **2013**, *56*, 6317-6329.

(17)   Klejnot, M.; Falnikar, A.; Ulaganathan, V.; Cross, R. A.; Baas, P. W.; Kozielski, F. *Acta Crystallogr. Sect. D. Biol. Crystallogr.* **2014**, *70*, 123-133.

(18)   Labriere, C.; Talapatra, S. K.; Thoret, S.; Bougeret, C.; Kozielski, F.; Guillou, C. *Bioorg. Med. Chem.* **2016**, *24*, 721-734.

(19)   Klejnot, M.; Kozielski, F. *Acta Crystallogr D Biol Crystallogr* **2012**, *68*, 154-159.

(20)   Bergnes, G.; Brejc, K.; Belmont, L. *Curr. Top. Med. Chem.* **2005**, *5*, 127-145.

(21)   Henderson, M. C.; Shaw, Y. J.; Wang, H.; Han, H.; Hurley, L. H.; Flynn, G.; Dorr, R. T.; Von Hoff, D. D. *Mol. Cancer Ther.* **2009**, *8*, 36-44.

(22)   Catarinella, M.; Gruner, T.; Strittmatter, T.; Marx, A.; Mayer, T. U. *Angew. Chem. Int. Ed. Engl.* **2009**, *48*, 9072-9076.

(23)   Tcherniuk, S.; Skoufias, D. A.; Labriere, C.; Rath, O.; Gueritte, F.; Guillou, C.; Kozielski, F. *Angew. Chem. Int. Ed. Engl.* **2010**, *49*, 8228-8231.

(24)   Aoki, S.; Ohta, K.; Yamazaki, T.; Sugawara, F.; Sakaguchi, K. *FEBS J.* **2005**, *272*, 2132-2140.

(25)   Wu, J.; Mikule, K.; Wang, W.; Su, N.; Petteruti, P.; Gharahdaghi, F.; Code, E.; Zhu, X.; Jacques, K.; Lai, Z.; Yang, B.; Lamb, M. L.; Chuaqui, C.; Keen, N.; Chen, H. *ACS Chem. Biol.* **2013**, *8*, 2201-2208.

(26)   Watts, C. A.; Richards, F. M.; Bender, A.; Bond, P. J.; Korb, O.; Kern, O.; Riddick, M.; Owen, P.; Myers, R. M.; Raff, J.; Gergely, F.; Jodrell, D. I.; Ley, S. V. *Chem. Biol.* **2013**, *20*, 1399-1410.

(27)   LoRusso, P. M.; Goncalves, P. H.; Casetta, L.; Carter, J. A.; Litwiler, K.; Roseberry, D.; Rush, S.; Schreiber, J.; Simmons, H. M.; Ptaszynski, M.; Sausville, E. A. *Invest. New Drugs* **2015**, *33*, 440-449.

(28)   Chung, V.; Heath, E. I.; Schelman, W. R.; Johnson, B. M.; Kirby, L. C.; Lynch, K. M.; Botbyl, J. D.; Lampkin, T. A.; Holen, K. D. *Cancer Chemother. Pharmacol.* **2012**, *69*, 733-741.

(29)   Luo, L.; Carson, J. D.; Dhanak, D.; Jackson, J. R.; Huang, P. S.; Lee, Y.; Sakowicz, R.; Copeland, R. A. *Biochemistry* **2004**, *43*, 15258-15266.

(30)   Cochran, J. C.; Sontag, C. A.; Maliga, Z.; Kapoor, T. M.; Correia, J. J.; Gilbert, S. P. *J. Biol. Chem.* **2004**, *279*, 38861-38870.

(31)   Kozielski, F.; DeBonis, S.; Skoufias, D. A. *Methods Mol. Med.* **2007**, *137*, 189-207.

(32)   Molnar, K.; Farkas, E. *Z. Naturforsch C.* **2010**, *65*, 157-173.

(33)   Bezivin, C.; Tomasi, S.; Rouaud, I.; Delcros, J. G.; Boustie, J. *Planta Med.* **2004**, *70*, 874-877.

(34)   Russo, A.; Piovano, M.; Lombardo, L.; Garbarino, J.; Cardile, V. *Life Sci* **2008**, *83*, 468-474.

(35)   Shrestha, G.; St. Clair, L. *Phytochemistry Reviews* **2013**, *12*, 229-244.

(36)   Elix, J. A.;A Catalogue of Standardized Chromatographic Data and Biosynthetic Relationships for Lichen Substances. Third Edition ed., 2014

(37)   Abdou, R.; Scherlach, K.; Dahse, H. M.; Sattler, I.; Hertweck, C. *Phytochemistry* **2010**, *71*, 110-116.

(38)   Morita, H.; Tsuchiya, T.; Kishibe, K.; Noya, S.; Shiro, M.; Hirasawa, Y. *Bioorg. Med. Chem. Lett.* **2009**, *19*, 3679-3681.

(39)   Chomcheon, P.; Wiyakrutta, S.; Sriubolmas, N.; Ngamrojanavanich, N.; Kengtong, S.; Mahidol, C.; Ruchirawat, S.; Kittakoop, P. *Phytochemistry* **2009**, *70*, 407-413.

(40)   Huneck, S.; Yoshimura, I. *Springer; New York* **1996**.

(41)   Wang, F.; Good, J. A.; Rath, O.; Kaan, H. Y.; Sutcliffe, O. B.; Mackay, S. P.; Kozielski, F. *J. Med. Chem.* **2012**, *55*, 1511-1525.

(42)   Kaan, H. Y.; Hackney, D. D.; Kozielski, F. *Science* **2011**, *333*, 883-885.

(43)   Hackney, D. D.; Jiang, W. *Methods Mol Biol* **2001**, *164*, 65-71.

(44)   Kaan, H. Y.; Ulaganathan, V.; Hackney, D. D.; Kozielski, F. *Biochem. J.* **2010**, *425*, 55-60.

(45)   McWilliam, H.; Li, W.; Uludag, M.; Squizzato, S.; Park, Y. M.; Buso, N.; Cowley, A. P.; Lopez, R. *Nucleic Acids Res.* **2013**, *41*, W597-600.

(46)   Kull, F. J.; Sablin, E. P.; Lau, R.; Fletterick, R. J.; Vale, R. D. *Nature* **1996**, *380*, 550-555.

(47)   Robert, X.; Gouet, P. *Nucleic Acids Res.* **2014**, *42*, W320-324.

TABLES

Table 1: *B*iochemical *C*haraterization of *M*PP1.[a]

enzyme	mass spec finger print [Coverage %]	gel filtration [MW kDa]	basal ATPase activity		MT-stimulated ATPase activity		
			k_{cat} [s^{-1}]	$K_{M,ATP}$ [µM]	k_{cat} [s^{-1}]	$K_{M,ATP}$ [µM]	$K_{0.5,MT}$ [nM]
MPP1$_{2-477}$	56	51	0.016 ± 0.001	68.5 ± 16	3.1 ± 0.2	44 ± 4	102 ± 3.2
MPP1$_{57-491}$	77	43	0.010 ± 0.001	128 ± 2.1	4.1 ± 0.1	82 ± 2	112 ± 1.0

[a] Initial biochemical characterization of two MPP1 constructs including mass spectrometry finger print analysis, gel filtration, and the determination oft he basal as well as MT-stimulated steady state ATPase activities.

Table 2: *I*nhibition of *M*PP1 by *D*epsidones.[a]

cmpd No (Name)	inhibition of basal ATPase activity $\text{MPP1}_{57\text{-}491}$ [µM] (MIA)	inhibition of MT-stimulated ATPase activity $\text{MPP1}_{57\text{-}491}$ [µM] (MIA)	inhibition of basal ATPase activity $\text{MPP1}_{2\text{-}477}$ [µM] (MIA)	inhibition of MT-stimulated ATPase activity $\text{MPP1}_{2\text{-}477}$ [µM] (MIA)
1 (norlobaridone)	18.7 ± 2.6 (75)	24.4 ± 3.5 (90)	10.8 ± 1.7 (80)	7.6 ± 0.7 (90)
2 (physodic acid)	9.9 ± 1.1 (85)	5.8 ± 0.9 (90)	10.4 ± 1.7 (90)	4.6 ± 0.8 (95)
3 (variolaric acid)	n.i.	n.i.	n.i.	n.i.

[a] Determination of IC_{50} values for the inhibition of the basal and MT-stimulated ATPase activity of two human MPP1 constructs, $\text{MPP1}_{57\text{-}491}$ and $\text{MPP1}_{2\text{-}477}$ by the three depsidones norlobaridone, physodic acid and variolaric acid from lichen. MIA: Maximum Inhibition Attained in percentage; n.i.: no inhibition.

Table 3: *Investigation of the Inhibitory Activity of Depsidones in Tumor Cell Lines.[a]*

cmpd no.	GI$_{50}$ [μM]				
	HCT116	J82	UM-UC-3	K562	BxPC-3
1	42.9 ± 8.4	48.3 ± 23.8	30.5 ± 3.5	43.7 ± 6.1	33.1 ± 3.8
2	>50	38.2 ± 10.6	31.8 ± 6.2	32.6 ± 2.3	37.3 ± 6.1
3	>100	>50	>100	>100	n.d.
4	0.8 ± 0.1	3.6 ± 0.3	3.7 ± 0.2	1.4 ± 0.1	1.6 ± 0.1

[a]Tumor cell lines from colon (HCT116), leukemia (K562) bladder (J82 and UM-UC-3) and pancreatic (BxPC3) cancer cell lines were used to test the inhibitory activity of the compounds. The Eg5 inhibitor STLC (**4**) was used as a control.

Table 4: *S*pecificity of *P*hysodic *A*cid.[a]

human kinesin	family	inhibition of basal ATPase activity IC_{50} [μM] (MIA)	inhibition of MT-stimulated ATPase activity, IC_{50} [μM] (MIA)
$MPP1_{57-491}$	kinesin-6	9.9 ± 1.1 (85)	5.8 ± 0.9 (90)
Kif15	kinesin-12	n.i.	n.i.
Eg5	kinesin-5	n.i.	n.i.
MKLP-1	kinesin-6	n.i.	40%
MKLP-2	kinesin-6	n.i.	n.i.
Kif7	kinesin-4	n.i.	n.i.
Kif27	kinesin-4	n.i.	n.i.
CENP-E	kinesin-7	29.6 ± 12.7 (70)	91.4 ± 31.0 (60)
Kif5A	kinesin-1	n.i.	n.i.
Kif5C	kinesin-1	n.i.	n.i.
Kif3B	kinesin-2	n.i.	40%
Kif9	kinesin-9	40%	50%
Kif4A	kinesin-4	40%	40%
Kif24	kinesin-13	n.i.	n.i.

[a]**2** was tested on the inhibition of the basal and MT-stimulated ATPase activities of a variety of human kinesins functionally involved in either mitosis or intracellular transport. Compounds were measured to a concentration of 200 μM. MIA: Maximum Inhibition Attained in percentage, n.i.: no inhibition.

Table 5: *P*rofiling of some basic *Drug-Like* properties.[a]

assay / compounds	1	2
molecular weight [Da]	398.45	470.19
turbidimetric solubility pH 2.0, 6.0, 7.4 [μM]	6.5, 3.75, 37.5	3.75, 65, >100
log $D_{7.4}$	3.5	3.0 ± 0.04
[%]clogP	6.9	6.9
PAMPA [Papp, 10^{-6} cm/s] mean recovery [%]	32.4 ± 5.3 95.1	low passive permeability 77.0
Caco-2 efflux ratio [Mean P_{app} B2A / Mean P_{app} A2B]	0.51	n.d. [*]low recovery
microsomal stability [Clint (μl/min/mg protein] $t_{1/2}$ [min] human	393 ± 9.1 3.5	310 ± 9.4 4.5
mouse	452 ± 21.9 3.1	61.6 ± 13.0 22.5
chemical stability	n.d.	stable

[a]n.d.: not determined. *Possible solubility or binding issues. [%] Calculated using Chemdraw.

FIGURE LEGENDS

Figure 1: Chemical structures of depsidones and a quinoxaline MPP1 inhibitor. **1** and **2** are inhibitors of MPP1 ATPase activity, whereas variolaric acid does not inhibit MPP1 activity. Corynesidone A (**5**) is a known aromatase inhibitor whereas lobaric acid (**4**) has been shown to inhibit MT polymerization. The quinoxaline analogue **6** has been shown to inhibit MPP1, although the patent has been withdrawn.

Figure 2: MPP1 domain organization and interactions. (A) Bar diagram of the human kinesin MPP1 and the two protein constructs used in this study. MPP1 has a small N-terminal domain of unknown function (aa 1-56) preceding the motor domain (aa 57-491). The motor domain contains an unusually long insertion in the loop L6 region, which is unique to kinesin-6 family members (marked with a yellow bar), and nucleotide-binding as well as MT interacting regions. The motor domain is followed by a stalk domain that is predicted to form a discontinuous coiled coil domain (aa 568-1600). The C-terminal domain (aa 1600-1853) predicted to be predominantly unfolded contains a phosphorylation site (Thr1644)[8] and the Pin1 interacting region. The two MPP1 constructs used in this study are $MPP1_{2-477}$ that covers the small N-terminal region and the entire motor domain, whereas $MPP1_{57-491}$ codes for the motor and the beginning of the neck-linker region. (B) Sequence and structure alignment of the human MPP1 motor domain and the motor domain of human Kif5B (conventional kinesin, kinesin-1) for which the crystal structure is available. The alignment shows the characteristic long inserting in the motor domain of MPP1 inserted in the loop L6 region (yellow) of the motor domain and also the N-terminal region (green), both of unknown function. The sequence alignment was performed using ClustalW at EMBL-EBI.[45] Secondary structure elements of the Kif5B motor domain were extracted from the coordinates of its crystal structure (PDB ID: 1BG2[46]) using ESPript 3.0.[47]

Figures 3: Characterization of the basal and MT-stimulated ATPase activity of two MPP1 constructs. (A) Effect of the NaCl concentration on the basal ATPase activity of $MPP1_{2-447}$ (□) and $MPP1_{57-491}$ (●) at saturating ATP concentration of 2 mM. (B) The basal ATPase activity for $MPP1_{2-447}$ (□) and $MPP1_{57-491}$ (●) in the presence of increasing ATP concentration from 0 to 2 mM, measured in the absence of salt (C) Determination of the MT-stimulated ATPase activity of $MPP1_{2-447}$ (□) and $MPP1_{57-491}$

($\bullet$) in the presence of increasing ATP concentrations in the range of 0 to 2 mM (D) MT-stimulated ATPase activity of MPP1$_{2-447}$ ($\square$) and MPP1$_{57-491}$ ($\bullet$) at increasing MT concentrations ranging between 0 and 10 μM .

**Figure 4:** Inhibition of MPP1$_{54-491}$ ATPase activity by depsidones. (A) Inhibition of basal ATPase activity of MPP1 by **2** ($\bullet$), **1** ($\blacklozenge$) and **3** ($\square$). (B) Inhibition of MT-stimulated ATPase activity of MPP1 by **2** ($\bullet$), **1** ($\blacklozenge$) and **3** ($\square$). In both basal and MT-stimulated ATPase assays **2** is more potent than **1**. Interestingly, the MPP1 ATPase activity is not inhibited by **3**, which unlike the other two depsidones miss the alkyl substituents in its chemical structure.

Figure 5: Determination of the type of inhibition for 2 with respect to ATP and MTs. (A) The type of inhibition determined in the absence of MTs at increasing ATP concentrations. **2** is uncompetitive inhibitor with respect to ATP as shown by ($\bullet$) 0 μM, ($\blacksquare$) 1 μM, ($\blacklozenge$) 5 μM, ($\blacktriangle$) 10 μM and ($\lozenge$) 20 μM of inhibitor at increasing concentrations of ATP. (B) The type of inhibition determined in the presence of 1 μM of MTs at increasing ATP concentrations. **2** shows mixed inhibition with respect to ATP even under MT-stimulated ATPase assay as shown by ($\bullet$) 0 μM, ($\blacksquare$) 1 μM, ($\blacklozenge$) 5 μM, ($\blacktriangle$) 10 μM and ($\lozenge$) 20 μM inhibitor at increasing concentrations of ATP. (C). **2** is a non-competitive inhibitor with respect to MTs: ($\bullet$) 0 μM, ($\blacksquare$) 1 μM, ($\blacklozenge$) 5 μM, ($\blacktriangle$) 10 μM and ($\lozenge$) 20 μM of inhibitor at increasing concentrations of MTs from 0 to 2 μM.
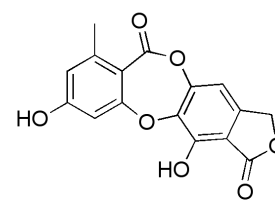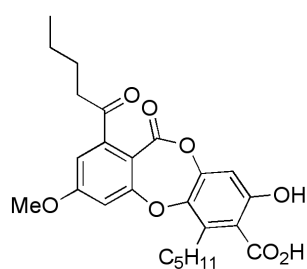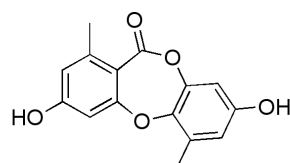
Figure 1
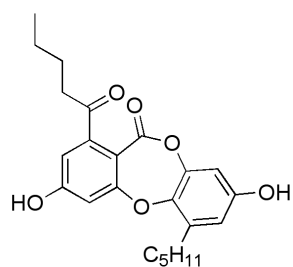
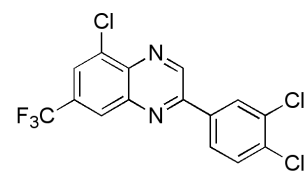norlobaridone
(**1**)
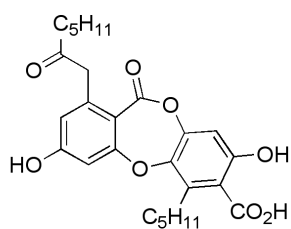
physodic acid
(**2**)

variolaric acid
(**3**)

lobaric acid
(**4**)

corynesidone A
(**5**)

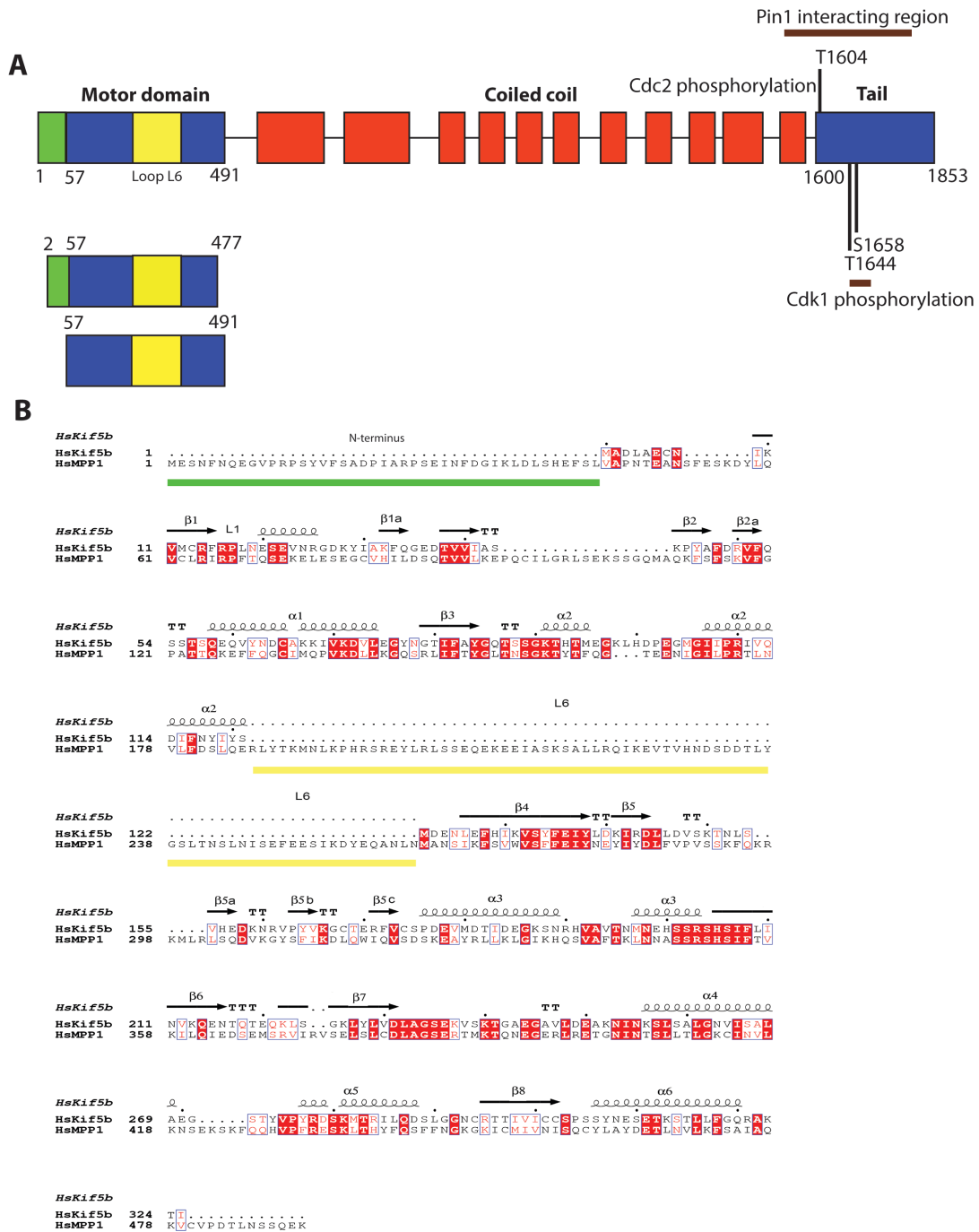5-chloro-2-(3,4-dichlorophenyl)-
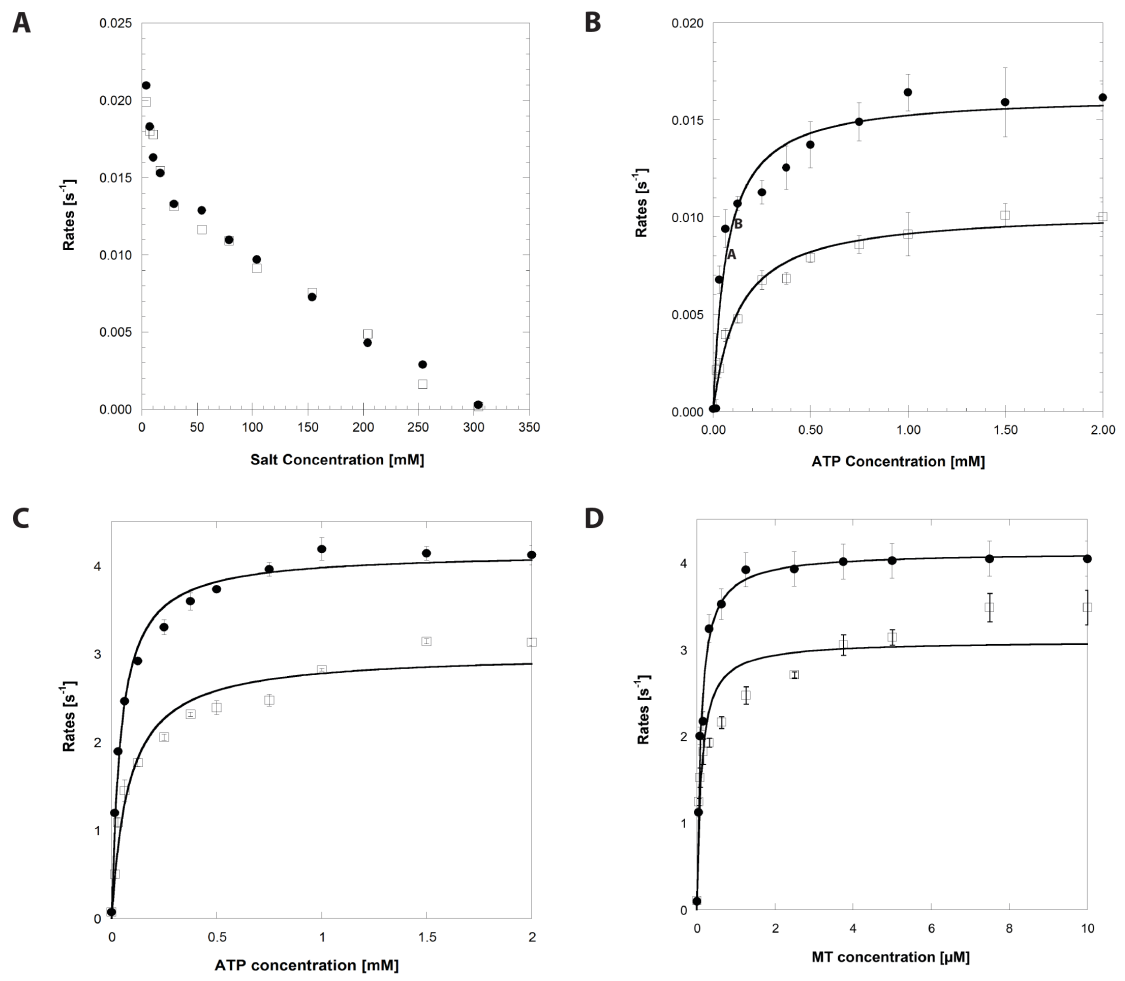7-(trifluoromethyl)quinoxaline
(**6**)

Figure 2

A

Pin1 interacting region

Motor domain   **Coiled coil**   Cdc2 phosphorylation   **Tail**

T1604

1   57   Loop L6   491

1600   1853

S1658
T1644

Cdk1 phosphorylation

2   57   477

57   491

B

```
HsKif5b                              N-terminus
HsKif5b     1  ..........................................................MADLAECN.......IK
HsMPP1      1  MESNFNQEGVPRPSYVFSADPIARPSEINFDGIKLDLSHEFSLVAPNTEANSFESKDYIQ

                  β1       L1                  β1a          TT                    β2      β2a
HsKif5b    11  VMCRFRPLNESEVNRGDKYIAKFQGEDTVVIAS................KPYAFDRVFQ
HsMPP1     61  VCLRIRPFTQSEKELESEGCVHILDSQTVVLKEPQCILGRLSEKSSGQMAQKFSFSKVFG

                  TT                  α1                    β3      TT      α2              α2
HsKif5b    54  SSTSQEQVYNDCAKKIVKDVLEGYNGTIFAYGQTSSGKTHTMEGKLHDPEGMGIIPRIVQ
HsMPP1    121  PATTQKEFPQGCIMQFVKDLLKGQSRLIFTYGLTNSGKTYTFQG...TEENIGILPRTLN

                  α2                                                    L6
HsKif5b   114  DIFNYITYS...................................................
HsMPP1    178  VIFDSLQERLYTKMNLKPHRSREYLRLSSEQEKEEIASKSALLRQIKEVTVHNDSDDTLY

                            L6                          β4         TT  β5      TT
HsKif5b   122  .........................MDENLEFHIKVSYFEIYLDKIRDILDVSKTNLS..
HsMPP1    238  GSLTNSLNISEFEESIKDYEQANLMANSIKFSVWVSFFEIYNFYIYDLFVPVSSKFQKR

                  β5a      TT  β5b  TT  β5c              α3                    α3
HsKif5b   155  ....VHEDKNRVPYVKGCTERFVCSPDEVMDTIDEGKSNRHVAVTNMNEHSSRSHSIPLI
HsMPP1    298  KMLRLSQDVKGYSFIKDLQWIQVSDSKEAYRLLKLGIKHQSVAFTKLNNASSRSHSIFTV

                  β6      TTT          β7            TT              α4
HsKif5b   211  NVKQENTQTEQKLS..GKLYLVDLAGSEKVSKTGAEGAVLDEAKNINKSLSALGNVISAL
HsMPP1    358  KILQIEDSEMSRVIRVSELSLCDLAGSERTMKTQNEGERLRETGNINTSLLTLGKCINVL

                                        α5                    β8              α6
HsKif5b   269  AEG.....STYVPYRDSKMTRILQDSLGGNCRTTIVICCSPSSYNESETKSTLFGQRAK
HsMPP1    418  KNSEKSKFQQHVPFRESKLTHYFQSFFNGKGKICMIVNISQCYLAYDETLNVLKFSAIAQ

HsKif5b   324  TI............
HsMPP1    478  KVCVPDTLNSSQEK
```
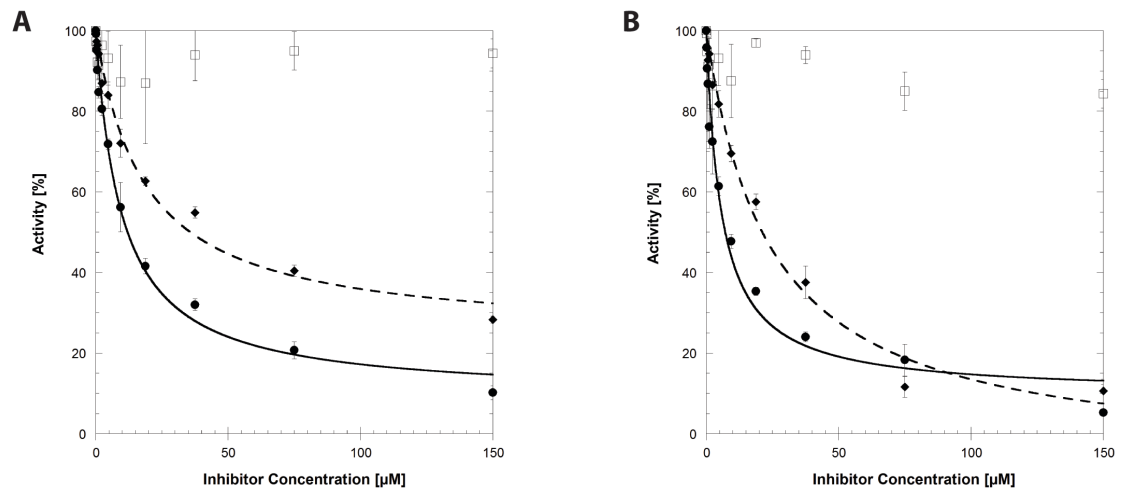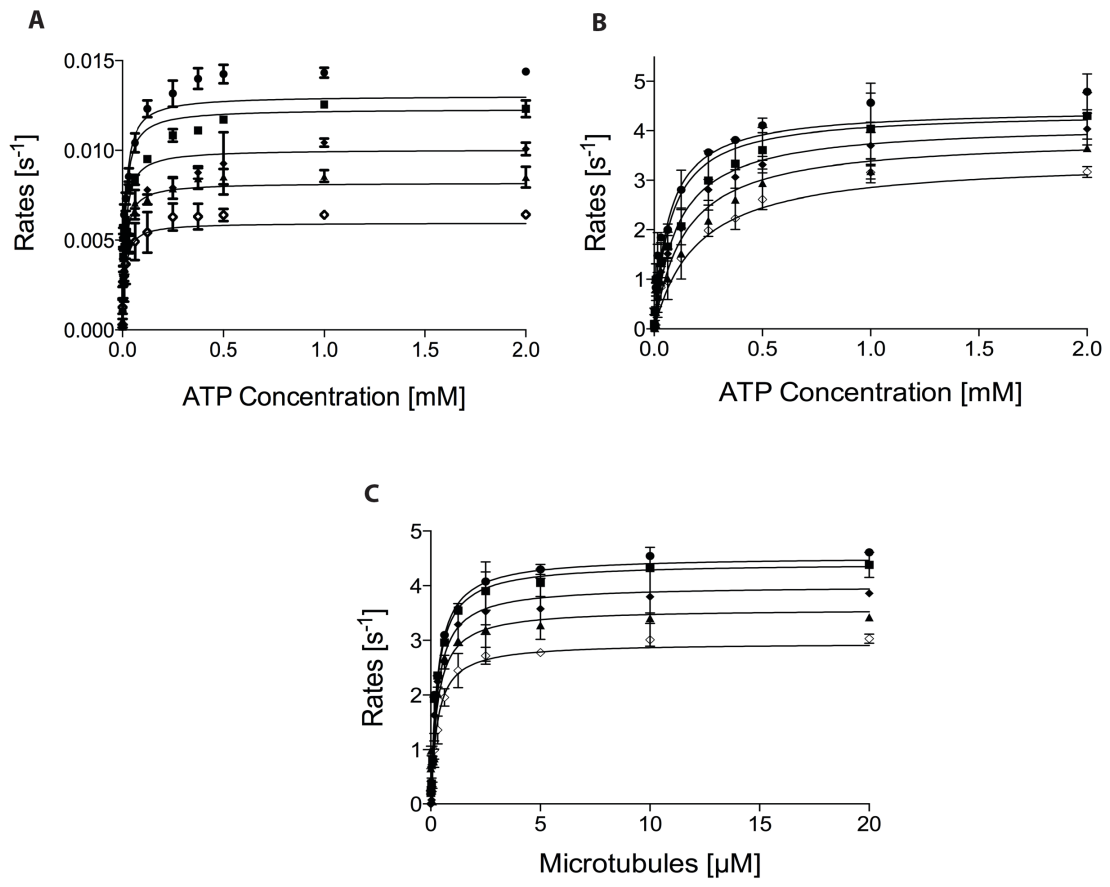
3

Figure 3

Figure 4

Figure 5

Table of Contents/Abstract Graphic

norlobaridone (1)
$IC_{50} = 18.7 \pm 2.6\ \mu M$

physodic acid (2)
$IC_{50} = 9.9 \pm 1.1\ \mu M$

MPP1 motor domain

Inhibition

7